Journal of Drug Targeting

http://informahealthcare.com/drt
ISSN: 1061-186X (print), 1029-2330 (electronic)

J Drug Target, 2013; 21(10): 968–980
 DOI: 10.3109/1061186X.2013.833207

informa
healthcare

ORIGINAL ARTICLE

Spacer length impacts the efficacy of targeted docetaxel conjugates in prostate-specific membrane antigen expressing prostate cancer

Zheng-Hong Peng[1], Monika Sima[1], Mohamed E. Salama[2], Pavla Kopečková[1], and Jindřich Kopeček[1,3]

[1]Department of Pharmaceutics and Pharmaceutical Chemistry/CCCD, [2]ARUP Reference Lab, and [3]Department of Bioengineering, University of Utah, Salt Lake City, UT, USA

Abstract

Combination of targeted delivery and controlled release is a powerful technique for cancer treatment. In this paper, we describe the design, synthesis, structure validation and biological properties of targeted and non-targeted *N*-(2-hydroxypropyl)methacrylamide (HPMA) copolymer-docetaxel conjugates. Docetaxel (DTX) was conjugated to HPMA copolymer via a tetrapeptide spacer (–GFLG-). 3-(1,3-dicarboxypropyl)-ureido]pentanedioic acid (DUPA) was used as the targeting moiety to actively deliver DTX for treatment of Prostate-Specific Membrane Antigen (PSMA) expressing prostate cancer. Short and long spacer DUPA monomers were prepared, and four HPMA copolymer – DTX conjugates (non-targeted, two targeted with short spacer of different molecular weight and targeted with long spacer) were prepared via Reversible Addition-Fragmentation Chain Transfer (RAFT) copolymerization. Following confirmation of PSMA expression on C4-2 cell line, the DTX conjugates' *in vitro* cytotoxicity was tested against C4-2 tumor cells and their anticancer efficacies were assessed in nude mice bearing *s.c.* human prostate adenocarcinoma C4-2 xenografts. The *in vivo* results show that the spacer length between targeting moieties and HPMA copolymer backbone can significantly affect the treatment efficacy of DTX conjugates against C4-2 tumor bearing nu/nu mice. Moreover, histological analysis indicated that the DUPA-targeted DTX conjugate with longer spacer had no toxicity in major organs of treated mice.

Keywords

C4-2, docetaxel, DUPA, HPMA, prostate cancer, PSMA, targeted drug delivery

History

Received 17 June 2013
Revised 5 August 2013
Accepted 6 August 2013
Published online 25 October 2013

Introduction

Prostate cancer (PCa) is the most common malignant cancer and the second leading cause of cancer-related death among men in the United States. It was estimated that 238 590 Americans will be newly diagnosed with prostate cancer and 29 720 Americans will die from prostate cancer in 2013 [1]. Although several therapeutic strategies, including radical prostatectomy, androgen deprivation, chemotherapy, bone-directed therapy and radiation therapy have been available for prostate cancer treatment, they are ineffective against advanced prostate cancer and also associated with severe side effects [1–3]. Docetaxel (Taxotere), the first line chemotherapy for prostate cancer treatment, is associated with fatigue, nausea or vomiting or both, alopecia, diarrhea, nail changes, sensory neuropathy, anorexia, changes in taste, stomatitis, dyspnea, tearing, peripheral edema and epistaxis [4]. One of the major reasons for these side effects is that DTX distributes indiscriminately into all cells of the body and causes damage to malignant and healthy cells alike. The significant mortality and morbidity of prostate cancer urgently require development of novel, safer and more potent formulations of DTX therapeutics. The recently developed nanomedicine technology can help to mitigate the off-target and dose limiting effects of small molecule therapeutics and enhance anti-tumor efficacy through polymer conjugate delivery system, especially decoration of the conjugate with a targeting ligand can provide the most effective therapy [5–10].

PSMA is a *Mr* 100 000 type II membrane protein containing a 19-amino acid (aa) cytoplasmic fragment, a single 24-aa membrane-spanning domain and a 707-aa extracellular region [11,12]. It has been exploited as an ideal target for treatment and diagnosis of prostate cancer because: (i) presented at the cell surface but not shed into the circulation; (ii) expressed about one thousand-fold higher in prostate cancer than the minimal expression seen in other tissues such as kidney, proximal small intestine, salivary gland [13]; (iii) increased expression with disease progression [14]. Therefore, several classes of ligands including aptamers [15–17], antibodies [18–21], peptides [22,23] and small molecules [24,25] have been developed to deliver therapeutics [26] and imaging agents [27–29] for treatment and diagnosis of PSMA expressing prostate cancer. Among them, small molecules are attractive due to their favorable

Address for correspondence: Jindřich Kopeček, University of Utah, Center for Controlled Chemical Delivery, 2030 East 20 South, Biopolymers Research Building, Room 205B, Salt Lake City, Utah 84112-9452, USA. Tel: +1 (801) 581-7211. Fax: +1 (801) 581-7848. E-mail: jindrich.kopecek@utah.edu

characteristics: multivalency, low cost, reproducible chemical synthesis, non-immunogenicity, high permeability in solid tumors and fast clearance from normal tissue.

Phosphoramidate and glutamate ureas are two major classes of small-molecule ligands that can bind PSMA selectively and with high affinity [24,25,30,31]. However, majority of their applications focus on imaging prostate cancer on murine models [27–29]. Few efforts have used small-molecule anti-PSMA ligands for treatment studies in mice models, maybe due to the challenging chemistry for small molecule ligands modification [26,32,33]. DUPA belongs to a class of glutamate ureas [24,25]; it is comparatively easy to modify the R group at C-2 position. We, therefore, reasoned that we might be able to incorporate a spacer at this position to connect the polymer-drug conjugate and DUPA targeting moiety.

The 3.5 Å resolution crystal structure of PSMA demonstrates that the active site of PSMA contains two zinc atoms coordinated by histidine and glutamate/aspartate residues [34]. Furthermore, Hilgenfeld's group demonstrated that the active binding site is accessible by a funnel-shaped tunnel with a depth of approximately 20 Å [35].

Based on the above considerations, we were interested in using DUPA as the targeting moiety to actively deliver DTX for treatment of PSMA expressing prostate cancer. DUPA and DTX were incorporated into the uncharged, hydrophilic and biocompatible HPMA copolymer via a suitable spacer length linker and lysosomally degradable spacer, respectively [8,36]. We hypothesized that conjugation of the targeting moiety DUPA to HPMA copolymer will enhance the ligands opportunity to bind to PSMA by increasing the circulation time of DUPA. The overall goal of the combination of targeted delivery and controlled release of DTX is to enhance its antitumor efficacy and lower its toxicity. Herein, we designed, synthesized and characterized polymerizable derivatives of DTX and DUPA (short and long spacer). We synthesized the DUPA-targeted or non-targeted HPMA copolymer - DTX conjugates and assessed their anticancer efficacies in nude mice bearing *s.c.* human prostate adenocarcinoma C4-2 xenografts. We also tested the toxicity of DTX conjugates by monitoring mice body weight changes and using a histological assay.

Materials and methods

Materials

DTX was purchased from AK Scientific (Union City, CA). *N*-(3-aminopropyl) methacrylamide (APMA) was purchased from PolySciences (Warrington, PA). Initiator 2,2′-azobis(2,4-dimethylvaleronitrile) (V-65) and azobisisobutyronitrile (AIBN) were purchased from Wako Pure Chemicals (Richmond, VA). L-glutamate di-*tert*-butyl ester hydrochloride, *O*-(7-azabenzotriazol-1-yl)-*N*,*N*,*N*′,*N*′-tetramethyluronium hexafluorophosphate (HATU), 4-dimethylaminopyridine (DMAP) and 1-ethyl-3-(3-dimethylaminopropyl)carbodiimide hydrochloride (EDC) were purchased from AAPPTec (Louisville, KY). L-glutamic acid γ-benzyl ester α-tert-butyl ester was purchased from Chem-Impex International (Wood Dale, IL). 1-(9H-fluoren-9-yl)-3-oxo-2,7,10,13,16,19,22,25,28,31,34,37,40-tridecaoxa-4-azatritetracontan-43-oic acid (Fmoc-NH-EG_{12}-COOH) was purchased from Peptides International (Louisville, KY). Monomer HPMA [37], *N*-methacryloyl-Gly-Phe-Leu-Gly-OH (MA-GFLG-OH) [38] and chain transfer agent 4-cyanopentanoic acid dithiobenzoate (CPAD) [39] were prepared as the literature described. All other reagents were purchased from Sigma Aldrich (St. Louis, MO) if not otherwise mentioned.

Synthesis of monomers

Synthesis of N-methacryloylglycylphenylalanylleucylglycyl docetaxel (MA-GFLG-DTX; Figure 1)

A solution of MA-GFLG-OH (920.5 mg, 2 mmol), DTX (807.4 mg, 1 mmol) and DMAP (146.6 mg, 1.2 mmol) in dichloromethane (DCM) (5 mL) was cooled to 0 °C in an ice bath, then EDC (230 mg, 1.2 mmol) was added at 0 °C. The reaction mixture was stirred at 0 °C for 2 h, then allowed to warm to room temperature and stirred at room temperature for additional 22 h. The reaction mixture was washed with water three times, brine once and dried over anhydrous sodium

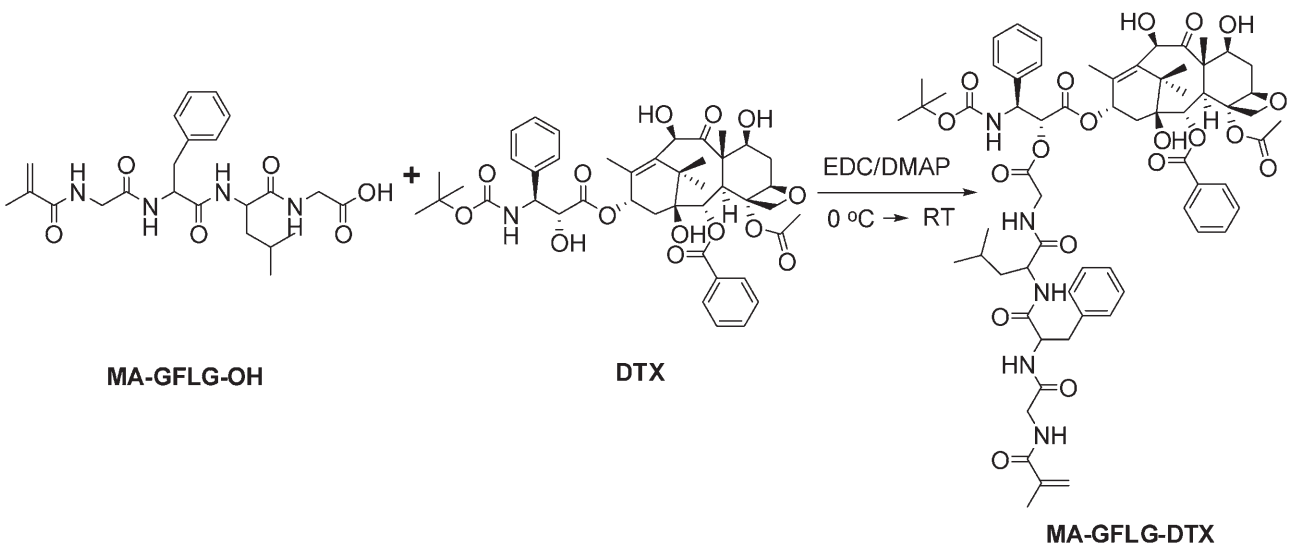

Figure 1. Synthetic scheme and structure of monomer MA-GFLG-DTX.

sulfate. After removing the solvent under reduced pressure, the crude residue was purified by column chromatography (silica gel 60 Å, 200–400 mesh; ethyl acetate: hexane = 1:4, 1:1, 100% ethyl acetate) to obtain 800 mg pure product with 64% yield. The structure of the product was validated by mass spectroscopy (Figure 1S). MALDI-MS: calcd for $C_{66}H_{83}N_5NaO_{19}$ ($[M+Na]^+$) 1273.4, found 1273.8; calcd for $C_{66}H_{83}N_5KO_{19}$ ($[M+K]^+$), 1289.5, found 1289.8.

Synthesis of (3S,7S)-17-methyl-5,10,16-trioxo-4,6,11,15-tetraazaoctadec-17-ene-1,3,7-tricarboxylic acid (MA-DUPA)

The synthesis procedure is schematically shown in Figure 2. Numbers of compounds used in the description below also relate to Figure 2.

*Synthesis of ((S)-5-benzyl 1-tert-butyl 2-(3-((S)-1,5-di-tert-butoxy-1,5-dioxopentan-2-yl)ureido) pentanedioate) (**4**).* To a dried three-neck flask was added L-glutamate di-*tert*-butyl ester hydrochloride (**1**; 2.5 g, 8.45 mmol) and 100 mL of DCM under nitrogen atmosphere. After the solution was cooled to −65 °C, triphosgene (**2**; 830 mg, 2.8 mmol) and 2.5 mL of triethylamine were added. Then this solution was stirred for 5 h and temperature gradually raised from −65 °C to 10 °C under the protection of nitrogen. The solution was re-cooled to −65 °C before adding a solution of L-Glu(OBn)-O^{t}Bu (**3**; 3 g, 9.1 mmol) and triethylamine (1.5 mL) in DCM (50 mL). The reaction mixture was allowed to increase to room temperature over a period of 2 h and stirred at room temperature overnight. The reaction was quenched with 1 M HCl, and the organic layer was washed with water, brine and dried over anhydrous sodium sulfate. The crude product was purified using flash chromatography to obtain 2.95 g (60.3%) of product as colorless oil.

*Synthesis of (S)-5-tert-butoxy-4-(3-((S)-1,5-di-tert-butoxy-1,5-dioxopentan-2-yl)ureido)-5-oxopentanoic acid (**5**).* ((S)-5-benzyl 1-tert-butyl 2-(3-((S)-1,5-di-tert-butoxy-1, 5-dioxopentan-2-yl)ureido) pentanedioate) (**4**; 1 g, 1.73 mmol) was dissolved in 30 mL of DCM, then 10% Pd/C (200 mg) was added into this solution. The reaction mixture was hydrogenated at 1 atm for 28 h at room temperature. Pd/C was filtered through a Celite pad and washed with DCM. The crude product was purified by using flash chromatography (silica gel; hexane: ethyl acetate = 4:1, 2:1, 1:1) to obtain the desired product as white solid (590 mg, 70% yield). The product was checked with ^{1}H NMR (Figure 2SA) and MS (Figure 2SB). ^{1}H NMR ($CDCl_3$) (Figure 2SA): δ 6.0 (d, J = 8.4 Hz, 1H); 5.52 (d, J = 8.4 Hz, 1H); 4.51–4.42 (m, 1H); 4.34–4.28 (m, 1H); 2.47–2.35 (m, 2H); 2.34–2.26 (m, 2H); 2.18–2.04 (m, 2H); 1.94–1.78 (m, 2H); 1.48 (s, 9H), 1.45 (s, 9H); 1.42 (s, 9H). HRMS (ESI+): calcd for $C_{23}H_{40}N_2O_9Na$ $[M+Na]^+$, 511.2631; found, 511.2643.

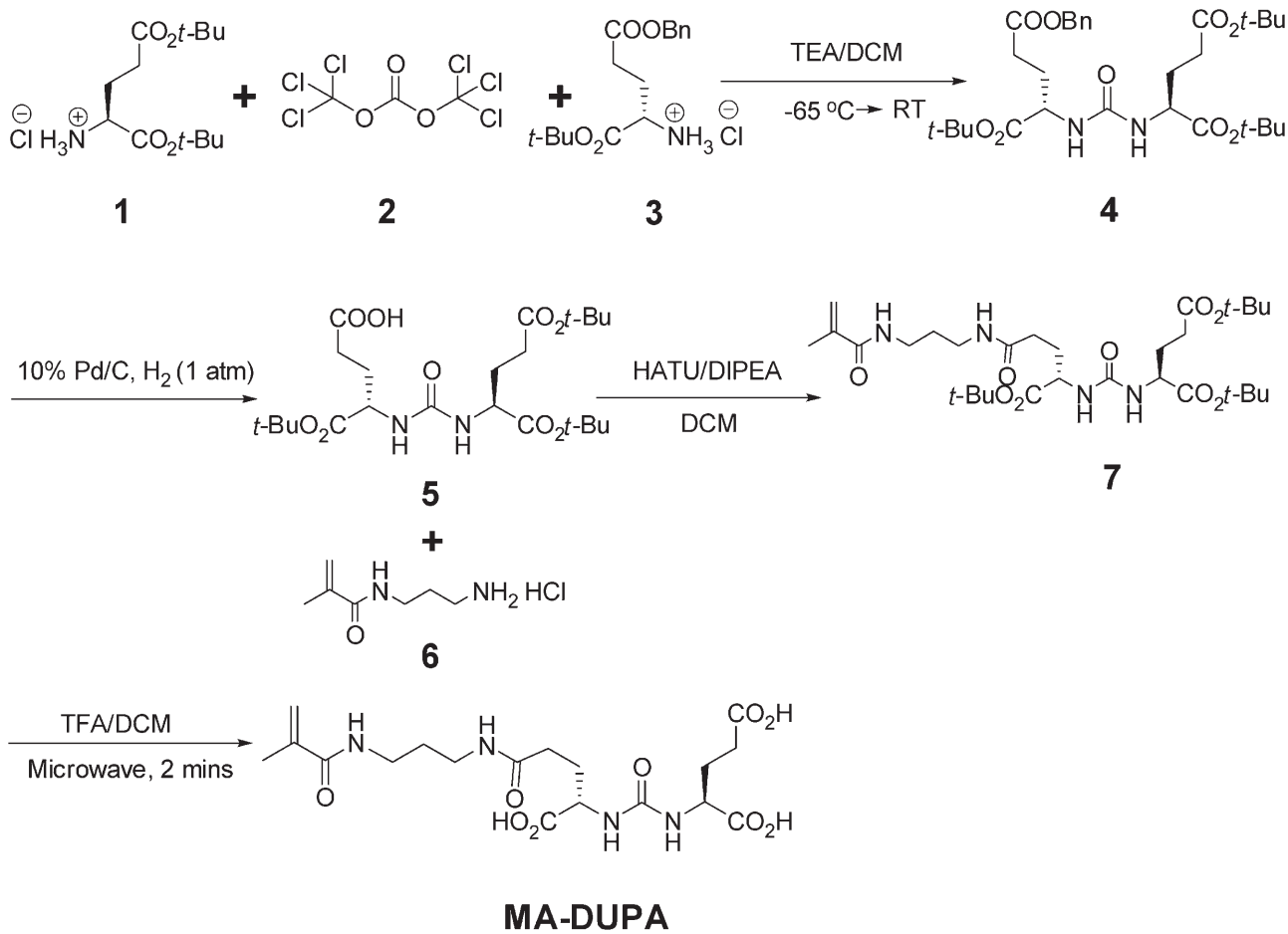

Figure 2. Synthetic scheme and structure of monomer MA-DUPA.

*Synthesis of (3S, 7S)-tri-tert-butyl 17-methyl-5,10,16-trioxo-4,6,11,15-tetraazaoctadec-17-ene-1,3,7-tricarboxylate (**7**).* (S)-5-tert-butoxy-4-(3-((S)-1,5-di-tert-butoxy-1,5-dioxopentan-2-yl)ureido)-5-oxopentanoic acid (**5**; 817 mg, 1.67 mmol), APMA (**6**; 329 mg, 1.84 mmol), HATU (700 mg, 1.84 mmol), *N*, *N*-diisopropylethylamine (DIPEA) (321 µL, 1.84 mmol) and DCM were added into 50 mL flask, then this mixture was stirred at room temperature overnight. Water was added into this mixture, the organic phase was washed with water and brine. Then the organic phase was dried over anhydrous sodium sulfate, filtered and concentrated under vacuum. The crude product was loaded on silica gel and was purified using flash chromatography (silica gel; hexane: ethyl acetate = 1:1; 100% of ethyl acetate; 30% methanol in DCM) to obtain 841 mg (yield = 82.2%) of product. The product was characterized with ^{1}H NMR (Figure 3SA) and MS (Figure 3SB). ^{1}H NMR (400 MHz, D_2O): δ 7.29 (t, $J = 6$ Hz, $J = 6.4$ Hz, 1H), 7.02 (t, $J = 6$ Hz, $J = 6.4$ Hz, 1H), 5.79 (s, 1H), 5.57 (d, $J = 8$ Hz, 1H), 5.47 (d, $J = 8$ Hz, 1H), 5.33 (s, 1H), 4.32–4.25 (m, 2H), 3.38–3.26 (m, 4H), 2.39–2.22 (m, 4H), 2.20–2.02 (m, 2H), 1.98 (s, 3H), 1.85–1.75 (m, 2H), 1.72–1.64 (m, 2H), 1.47 (s, 9H), 1.44 (s, 9H); 1.42 (s, 9H). HRMS (ESI+): calcd for $C_{30}H_{52}N_4O_9Na$ $[M + Na]^+$, 635.3632; found, 635.3641.

*Deprotection of compound **7** to produce MA-DUPA.* To a microwave reaction tube was added (3S, 7S)-tri-*tert*-butyl 17-methyl-5,10,16-trioxo-4,6,11,15-tetraazaoctadec-17-ene-1,3,7-tricarboxylate (**7**; 150 mg, 0.245 mmol), 1 mL of DCM, 2 mL of trifluoroacetic acid and stirrer bar. The tube was sealed and subjected to microwave irradiation (Biotage, Charlotte, NC) at 70 °C (150 W) for 2.5 min. After being cooled to room temperature and concentrated under reduced pressure, the crude product was precipitated in diethyl ether. After being dried under air and purified with HPLC, 79.3 mg (72.9%) of pure product was obtained. The product was characterized with ^{1}H NMR (Figure 3A) and MS (Figure 3B). ^{1}H NMR (400 MHz, D_2O): δ 5.51 (s, 1H), 5.27 (s, 1H), 4.10 (dd, $J = 9.2$ Hz, 5.2 Hz, 1H), 4.03 (dd, $J = 9.2$ Hz, 4.4 Hz, 1H), 3.10 (*t*, $J = 7.2$ Hz, 2H), 3.05 (*t*, $J = 6$ Hz, 2H), 2.35 (*t*, $J = 6$ Hz, 2H), 2.20 (*t*, $J = 6.8$ Hz, 2H), 2.08–1.96 (m, 2H), 1.86–1.76 (m, 2H), 1.75 (s, 3H), 1.60–1.52 (m, 2H). MS (ESI+): calcd for $C_{18}H_{28}N_4NaO_9$ ($[M + Na]^+$) 467.2, found 467.3.

Synthesis of (3S,7S)-57-methyl-5,10,50,56-tetraoxo-14,17,20, 23,26,29,32, 35,38,41,44,47-dodecaoxa-4,6,11,51,55-pentaazaoctapentacont-57-ene-1,3,7-tricarboxylic acid (MA-EG$_{12}$-DUPA)

The synthesis procedure is schematically shown in Figure 4. Numbers of compounds used in the description below also relate to Figure 4.

Synthesis of 1-amino-N-(3-methacrylamidopropyl)-3,6,9,12,15,18,21,24, 27,30,33,36-dodecaoxanonatriacontan-39-amide (MA-EG$_{12}$-NH$_2$). To a carefully dried three-neck flask was added Fmoc-NH-EG$_{12}$-COOH (**8**; 90 mg, 0.11 mmol), HATU (82 mg, 0.22 mmol) and 2 mL DCM, and then the mixture was stirred for about 2 h. Then APMA (**6**; 38 mg, 0.22 mmol) and DIPEA (56 µL, 0.33 mmol) were

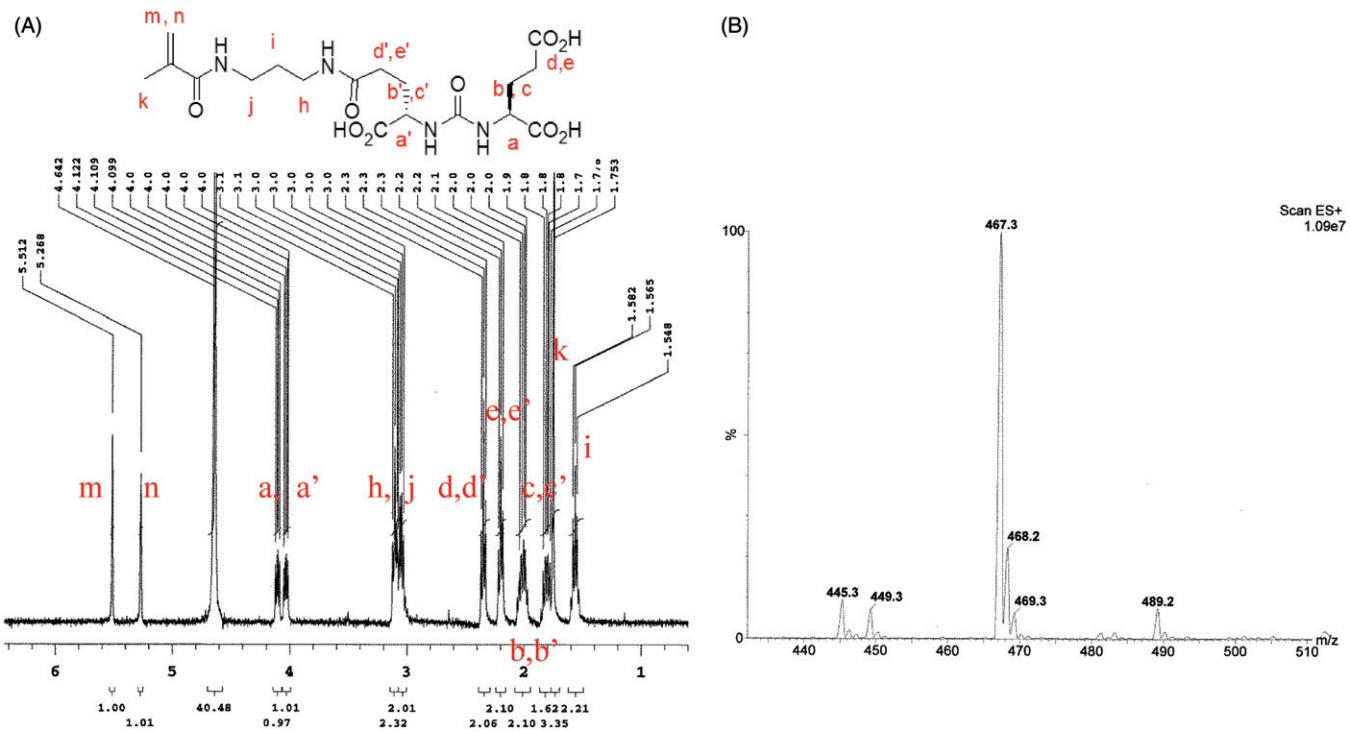

Figure 3. ^{1}H NMR and mass spectra of MA-DUPA.

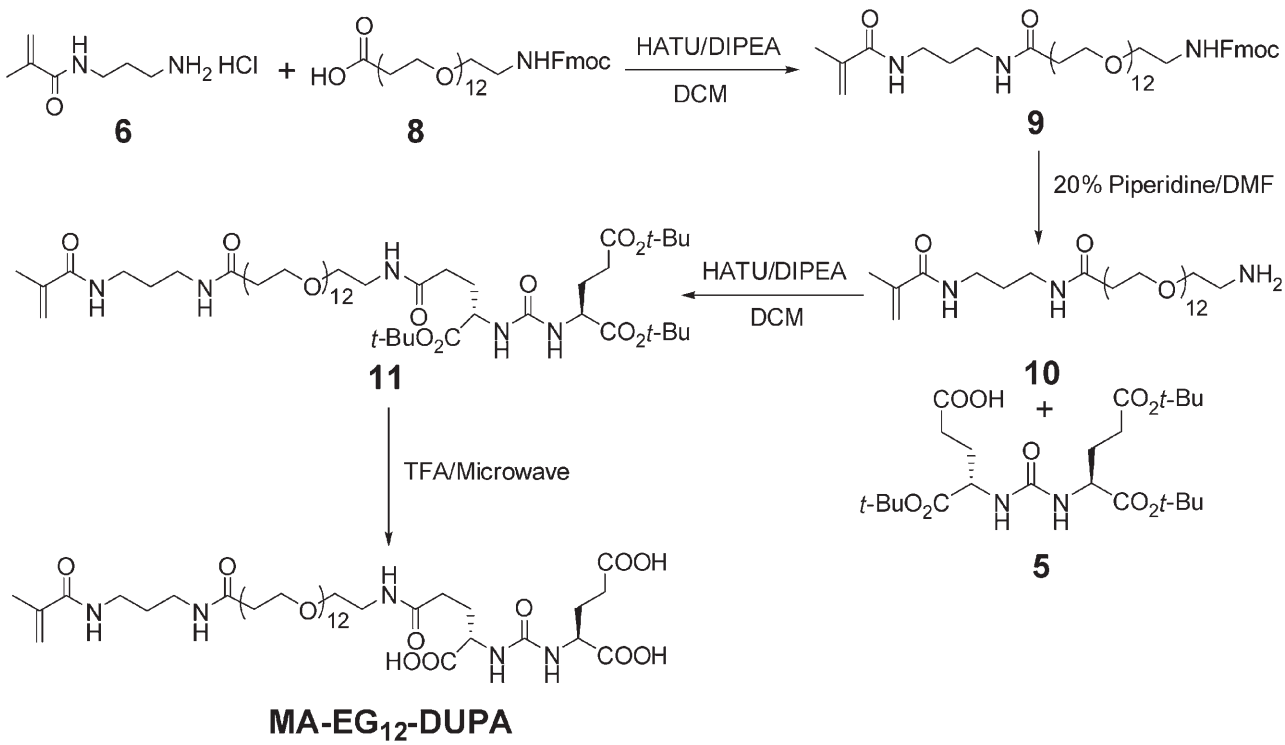

Figure 4. Synthetic scheme and structure of monomer MA-EG_{12}-DUPA.

added and stirred overnight. The crude product was washed with water three times, brine once and dried over anhydrous sodium sulfate. The product MA-EG_{12}-NHFmoc (**9**, 43 mg) was obtained with a yield 41%.

The obtained 43 mg of MA-EG_{12}-NHFmoc was re-dissolved in a mixture of DMF (1 mL) and piperidine (0.25 mL), then this mixture was stirred at room temperature for about 8 h. After removing the solvent, the remaining crude product was purified with flash chromatography on silica gel using methanol/DCM as eluent to provide the product MA-EG_{12}-NH_2 (**10**; 10 mg, 33%).

*Synthesis of (3S,7S) tri-tert-butyl 57-methyl-5,10,50,56-tetraoxo-14,17,20, 23,26,29,32,35,38,41,44,47-dodecaoxa-4,6,11,51,55-pentaazaoctapenta-cont-57-ene-1,3,7-tricarboxylate (MA-EG_{12}-DUPA(tri-tert-butyl); **11**).* To a carefully dried three-neck flask was added (S)-5-tert-butoxy-4-(3-((S)-1,5-di-tert-butoxy-1,5-dioxopentan-2-yl)ureido)-5-oxopentanoic acid (**5**; 658.5 mg, 1.35 mmol), HATU (512.4 mg, 1.35 mmol) and 2 mL DCM, the mixture was stirred for about 30 min. Then MA-EG_{12}-NH_2 (**10**; 500 mg, 0.67 mmol) and DIPEA (352 μL, 2.02 mmol) were added and stirred overnight. After removing the solvent, the crude product was purified with silica gel column with gradient solvent to afford 600 mg of desired products with the yield of 81.3%. The product was characterized with mass spectroscopy (Figure 4S). TOF-MS (ESI+): calcd for $C_{57}H_{106}N_5O_{22}$ ($[M+H]^+$), 1212.7, found 1212.8; calcd for $C_{57}H_{109}N_6O_{22}$ ($[M+NH_4]^+$), 1229.8, found 1229.8; calcd for $C_{57}H_{105}N_5NaO_{22}$ ($[M+Na]^+$), 1234.7, found 1234.7.

*Deprotection of compound **11** to produce MA-EG_{12}-DUPA.* MA-EG_{12}-DUPA(tri-*tert*-butyl) (**11**; 100 mg, 0.082 mmol) in 3 mL of a mixture of solvent (DCM/TFA = 1/2) was kept in a microwave reaction sealed tube. After being pre-stirred for 30 s, the reaction was conducted at 50 °C for 2 min in microwave reactor. After removing the solvent under reduced pressure, the remaining crude product was precipitated in diethyl ether. After being purified with semi-preparative HPLC, 42 mg of pure product was obtained in 48.8% yield. The product was characterized with mass spectroscopy (Figure 5). ESI: calcd for $C_{45}H_{80}N_5O_{22}$ ($[M-H]^-$), 1042.5. Found: 1042.5.

Preparation of DUPA-targeted and non-targeted HPMA copolymer-DTX conjugates with RAFT polymerization

Four DUPA-targeted and non-targeted HPMA copolymer-DTX conjugates (P-DTX, P-DTX-DUPA, P-DTX-mDUPA, P-DTX-EG_{12}-DUPA) were prepared with RAFT polymerization. The general procedure is demonstrated by the synthesis of P-DTX-EG_{12}-DUPA, a DUPA-targeted HPMA copolymer-DTX conjugate containing the long spacer: (i) monomer HPMA (238.7 mg, 1.667 mmol), MA-EG_{12}-DUPA (100 mg, 0.096 mmol) and MA-GFLG-DTX (56.7 mg, 0.045 mmol) were added into an ampoule; (ii) a solution of 0.9 mg CPAD in DMSO and 0.167 mg of V-65 in DMSO was added; (iii) more of DMSO and DI water were added until the final volume of DMSO was 1.8 mL and final volume of DI water was 1.2 mL; (iv) the mixture with nitrogen was bubbled for 30 min before sealing the ampoule; (iv) the RAFT copolymerization was conducted at 52 °C for 36 h. The resulting copolymer was precipitated in diethyl ether and purified by preparative FPLC. After freeze-drying, 138 mg of product was obtained (35% in yield).

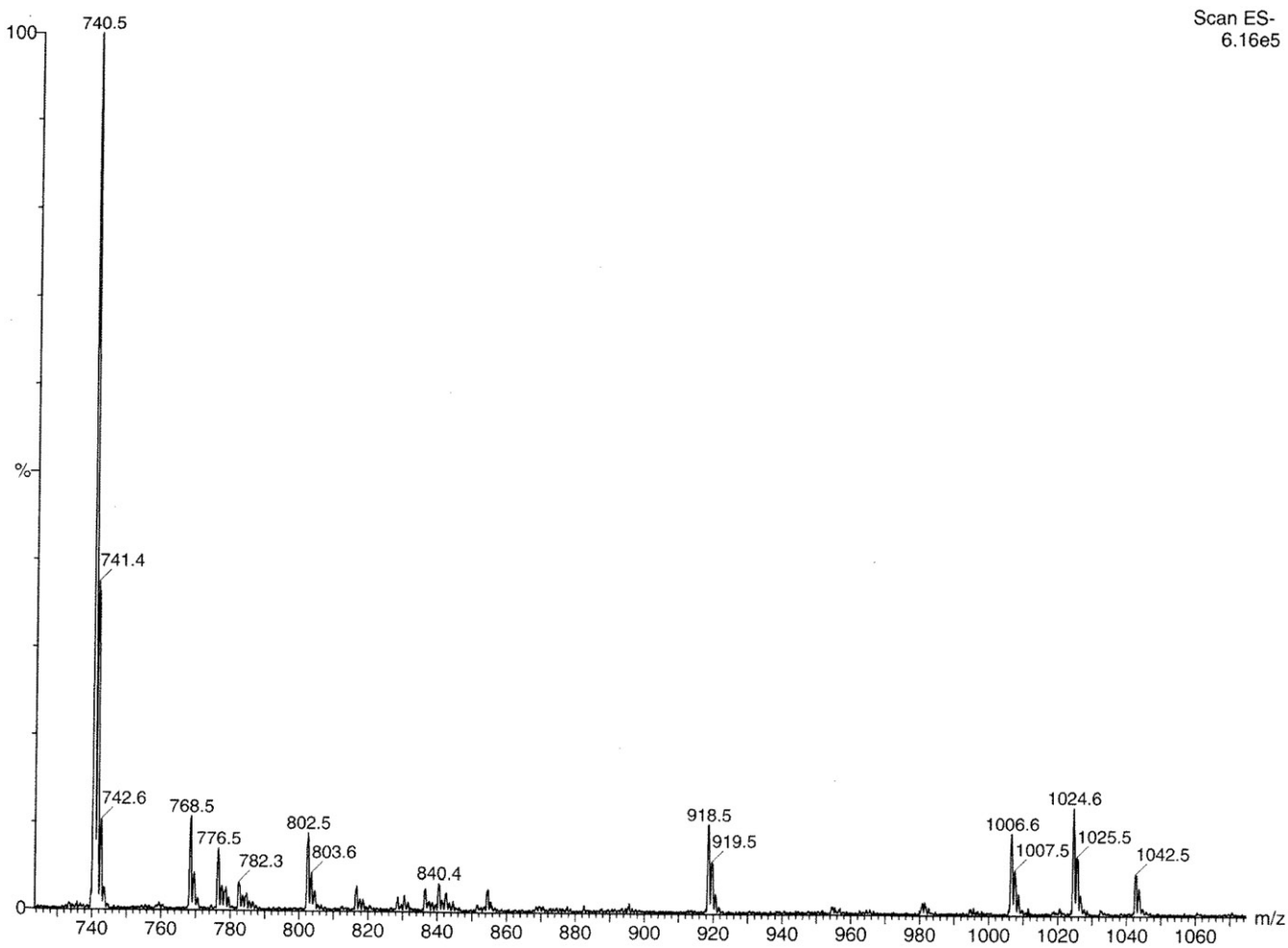

Figure 5. Mass spectrum of monomer MA-EG$_{12}$-DUPA.

Characterization of DUPA-targeted and non-targeted HPMA copolymer-DTX conjugates

The number average molecular weight (M_n), weight average molecular weight (M_w) and polydispersity (M_w/M_n) of DUPA-targeted or non-targeted HPMA copolymer-DTX conjugates were analyzed by size exclusion chromatography using a Superose 6 HR10/30 analytical column on an AKTA FPLC system (Pharmacia) equipped with refractive index (Optilab rEX) and light scattering MiniDawn TREOS detectors (Wyatt Technology Inc, Santa Barbara, CA). The buffer with 0.1 M of sodium acetate in a mixture of 30% acetonitrile/70% DI water (v/v) (pH = 6.5) was used as the eluant, and the flow rate was 0.4 mL/min. HPMA homopolymer fractions were used as molecular weight standards.

The DTX content in DUPA-targeted or non-targeted HPMA copolymer-DTX conjugates were determined by using HPLC after complete enzymatic hydrolysis of DTX from DUPA-targeted or non-targeted HPMA copolymer-DTX conjugates with excess of papain. The general procedure to measure the DTX content in conjugate: (i) to a 1 mL of Eppendorf vial was added 10 μL of 20 mg/mL of DTX conjugate in DMSO solution; (ii) 100 μL of 10 mM glutathione was added in Mcllvaine's buffer (50 mM citrate/0.1 M phosphate pH 6.0); (iii) 20 μL of 25 mg/mL papain was added in Mcllvaine's buffer (50 mM citrate/0.1 M phosphate pH 6.0); (iv) the mixture was incubated at 37 °C for 12 h; (v) the reaction was terminated by addition of 10 μL of 3×10^{-3} M sodium iodoacetate (enzyme inhibitor) solution and 280 μL of 0.02% of acetic acid in methanol. The amount of released DTX in the final mixture was measured by analytical HPLC (Agilent Technologies 1100 series, Zorbax C8 column 4.6×150 mm) using gradient elution from 30 to 90% of buffer B in 30 min (Buffer A: 0.1% TFA in DI water; Buffer B: 0.1% TFA in acetonitrile), and the flow rate was 1.0 mL/min. Free DTX was used for standard curve calibration generated under the same conditions as the assay.

The DUPA content in DUPA-targeted HPMA copolymer-DTX conjugates was determined by amino acid analysis. The general procedure for measuring DUPA content in DUPA-targeted HPMA copolymer-DTX conjugates: (i) 2 mg of DUPA-targeted HPMA copolymer-DTX conjugates and 0.5 mL of 6 M HCl in a sealed ampule were heated at 110 °C for 24 h, (ii) the solvent was removed under reduced pressure and the residue was re-dissolved in 100 μL of DI water; (iii) derivatization of hydrolyzed amino acid by sequential addition: 20 μL of potassium tetraborate in distilled water (150 μg/μL), 20 μL of o-phthaldialdehyde in methanol (50 μg/μL), 20 μL of mercaptopropionic acid in distilled water (0.05 mL/1 mL), 20 μL of sample solution; (iv) the mixture

Table 1. Physicochemical properties of DUPA-targeted and non-targeted DTX conjugates.

DTX conjugate	Spacer length	Mn (kDa)	Mw (kDa)	Mw/Mn	DTX (wt%)	DUPA units per polymer chain
P-DTX	N/A	50	59	1.18	5.30	N/A
P-DTX-DUPA	Short	48	64	1.34	5.86	7.9
P-DTX-mDUPA	Short	115	142	1.24	3.93	26.5
P-DTX-EG_{12}-DUPA	Long	70	81	1.16	3.84	4.8

was vortexed for 1 min and 0.5 mL of 0.1 M sodium acetate buffer was added, and then filtered; (v) the fluorescence ($E_x = 229$ nm, $E_m = 450$ nm) of the hydrolyzed amino acid derivatives was measured by analytical HPLC (Agilent Technologies 1100 series, XDB-C8, 5 μm, column 4.6 × 150 mm) using gradient elution (0–2 min, 10% buffer B; 2–10 min, 10–50% buffer B; 10–20 min, 50–60% buffer B; 20–25 min, 60% buffer B; 25–30 min, 60–70% buffer B; 30–35 min, 70–90% buffer B; 35–40 min, 90% buffer B) (Buffer A: 0.05 M sodium acetate in 25 mL of acetonitrile and 975 mL of DI water, pH 6; Buffer B: 0.05 M sodium acetate in 300 mL of DI water and 700 mL of methanol, pH 6), and the flow rate was 1.0 mL/min. Monomer MA-DUPA was used for standard curve calibration. The characteristics of synthesized conjugates are summarized in Table 1.

Cell culture

LNCaP-derived androgen-independent C4-2 cell line was provided by Dr Elsässer-Beile (University of Karlsruhe). PC-3 cell line was purchased from American Type Culture Collection (ATCC) (Manassas, VA). Cells were maintained in RPMI-1640 medium (Sigma-Aldrich, St. Louis, MO) supplemented with 10% (v/v) FBS, 100 Units/ml penicillin and 100 μg/mL streptomycin (Gibco, Carlsbad, CA). Cells were incubated at 37 °C in a humidified atmosphere of 5% CO_2 (v/v). Cells were passaged every 3–4 d and stopped at passage 20.

PSMA cell surface expression

The PSMA surface expression on C4-2 and PC-3 cells was measured by flow cytometry. The cells were detached from flask with 0.05% of trypsin in EDTA, centrifuged at 1000 rpm and washed three times with PBS. After cooling the cells and solutions to 4 °C, about 200 000 cells were re-suspended in 100 μL staining buffer (PBS solution containing 3% FBS and 0.1 % NaN_3). Then to each vial 100 μL of 10 μg/mL primary antibody 3 F/11 was added (provided by Dr Elsässer-Beile). The final 3/F11 concentration was 5 μg/mL. After being incubated for 30 min at 4 °C, the cells were washed three times with 1 mL of staining buffer. Following incubation with a 1:500 dilution of secondary antibody (Alexa Fluor 488 goat anti-mouse IgG (H + L), 4 μg/mL) (Life Technologies, Grand Island, NY) at 4 °C for 30 min, the cells were washed three times with staining buffer and kept in 250 μL of staining buffer for flow cytometry study. No-staining cells were used as the negative control.

In vitro cytotoxicity

The cytotoxicity of DTX conjugates against C4-2 human prostate cancer cells was measured by Cell Counting Kit-8 assay (CCK-8, Dojindo, Japan). The C4-2 cells were seeded in 96-well plates at a density of 5000 cells/well in 100 μL RMPI-1640 media containing 10% fetal bovine serum. After 24 h, old media were removed and replaced with a series concentration of DTX conjugates in 100 μL media. After 72 h, 50 μL of 1:5 diluted original CCK-8 solution was added and incubated for 1–2 h. The absorbance of the reduced product formazan at 450 nm (630 nm as reference) was measured with a microplate reader (Bio-Rad, Hercules, CA). The data were analyzed using GraphPad Prism v. 5.03 (GraphPad Software Inc., La Jolla, CA).

Tumor models

All animals were handled in compliance with the Institutional Animal Care and Use Committee (IACUC) guidelines in University of Utah. All works were conducted under the protocol (#10-10006) approved by University of Utah IACUC. Male nu/nu mice (about 6 weeks of age) were obtained from Charles River (Wilmington, MA) and housed in BPRB Rm#28 with a controlled environment (24 °C); 12:12-h light dark cycle under specific pathogen-free conditions with water and food provided *ad libitum*. In this study, male nu/nu mice were inoculated subcutaneously with two millions of C4-2 cells in 200 μL of a mixture of Matrigel/medium = 1/1 in the right flank.

In vivo anticancer efficacy of DUPA-targeted and non-targeted HPMA copolymer-DTX conjugates

The efficacies of DTX conjugates were assessed in six groups of nu/nu mice bearing C4-2 prostate cancer xenografts. When the tumor volume reached approximately 100–200 mm^3, the mice were administered three dosages of 3 mg/kg DTX equivalent DUPA-targeted and non-targeted HPMA copolymer-DTX conjugates, free DTX and saline via tail vein once per week (days 0, 7 and 14). After the first dose, the mice weight was monitored everyday and tumor growth was monitored three times per week. The perpendicular diameters (length and width) of the tumors were measured by digital calipers, and the tumor volume was calculated by the following formula: (3.14*$Width^2$*Length)/6. Mice were euthanized when the tumor weight reached 10% of the pre-dosing weight. Individual tumor volume relative to initial size was calculated. At study end points, mice were euthanized and their tumors as well as organs were excised. The tumors and organs were stored in 10% of formalin and embedded in paraffin, cryosectioned and stained with hematoxylin and eosin (H&E) for histological analysis. The slices were examined with fluorescence microscope.

Statistical analysis

Data values were expressed as the mean ± standard error of the mean (SEM). Difference between means was assessed by

one-way ANOVA and Dunnett's test using GraphPad Prism software. p Values ≤ 0.05 were considered statistically significant.

Results and discussion

Design, synthesis and characterization of polymerizable derivative of DTX (MA-GFLG-DTX)

There are two common ways to prepare drug conjugates: one way is to prepare the conjugate precursor first, then attach the drug into the conjugate; the other way is to prepare a monomer form of drug, then copolymerize with comonomers to prepare the drug conjugates. Compared with the former method, the latter method has several advantages: (i) flexible to control the drug content by adjusting the monomer drug content in feed; (ii) easier to obtain the pure product when the drug has several reactive groups. As there are three hydroxyl groups in DTX at the C-7, C-10 and C-2′ positions, respectively, we prefer to prepare monomer MA-GFLG-DTX first and then polymerize the comonomers. The tetrapeptide (–GFLG–) was used as the spacer to conjugate the drug DTX into HPMA copolymer as this peptide is degraded in the lysosomes [38,40,41]. Thus the free drug DTX will be released from the HPMA copolymer in the lysosomal compartment. The design and synthesis of MA-GFLG-DTX is shown in Figure 1. The monomer MA-GFLG-DTX was prepared by coupling MA-GFLG-OH [38] with DTX at 0 °C in the presence of DMAP and EDC in DCM. The coupling reaction occurred preferentially at the C-2′ hydroxyl position since the steric hindrance reduces the hydroxyl group reactivity at both C-7 and C-10 positions. Furthermore, the coupling reaction selectivity among those hydroxyl groups was enhanced by lowering the reaction temperature to 0 °C. The mass spectrum of MA-GFLG-DTX is shown in Supplementary Data (Figure 1S).

Design, synthesis and characterization of polymerizable DUPA derivatives with different spacer lengths

Using similar rationale as for MA-GFLG-DTX, the targeting moiety DUPA was also converted to a polymerizable form. We designed and synthesized two kinds of DUPA monomer, MA-DUPA (Figure 2) and MA-EG_{12}-DUPA (Figure 4). As the modification at C2 position in DUPA results in minimal loss of binding affinity [33], the monomer forms of DUPA were prepared by conjugation at this position. To make sure the targeting moiety can reach the active site of PSMA, we incorporated 12 ethylene glycol units as a spacer between the DUPA and methacryloyl group in the monomer MA-EG_{12}-DUPA. This >47 Å spacer should be long enough to easily access the PMSA binding site via the funnel-shaped tunnel [35]. To evaluate whether the spacer length between targeting moiety and polymer drug carrier can affect the efficacy of drug conjugates, we prepared monomer MA-DUPA with short spacer as a control.

The preparation of monomer (MA-DUPA) is shown in Figure 2. The core ligand, 2-[3-(1,3-bis-*tert*-butoxycarbonyl-propyl)-ureido] pentanedioic acid 1-*tert*-butyl ester, was synthesized according to the literature [24]. It started from reaction of L-glutamate di-*tert*-butyl ester hydrochloride, triphosgene and γ-benzoylated glutamic acid to obtain 2-[3-(3-benzyloxycarbonyl-1-*tert*-butoxycarbonyl-propyl)-ureido] pentanedioic acid di-*tert*-butyl ester (Compound **4**). The benzyl group was selectively removed with activated palladium-carbon to obtain the 2-[3-(1,3-bis-*tert*-butoxycarbonyl-propyl)-ureido] pentanedioic acid 1-*tert*-butyl ester (**5**). Then the carboxylic acid **5** was coupled with APMA to obtain (3 S, 7 S)-tri-*tert*-butyl 17-methyl-5,10,16-trioxo-4,6,11,15-tetraazaoctadec-17-ene-1,3,7-tricarboxylate (**7**). Under acid assisted microwave irradiation, three *tert*-butyl groups in compound **7** were removed to obtain monomer MA-DUPA. After being purified with RP-HPLC, the monomer MA-DUPA was characterized with both ^{1}H NMR and MS (Figure 3).

As shown in Figure 4, the preparation of monomer MA-EG_{12}-DUPA started from the coupling of APMA with Fmoc-NH-EG_{12}-COOH in the presence of HATU and DIPEA in DCM. After the Fmoc group in the MA-EG12-NHFmoc was removed with 20% piperidine in DMF, the amine **10** was coupled with carboxylic acid **5** to obtain MA-EG_{12}-DUPA(tri-*tert*-butyl). The next step is to remove the three *tert*-butyl groups. First, we tried the same reaction condition as used in the preparation of monomer MA-DUPA. From the mass spectrum, several water molecules were lost from the desired product. Then we optimized the reaction condition by lowering the reaction temperature from 70 °C to 50 °C. After being purified with RP-HPLC, the desired product MA-EG_{12}-DUPA with correct mass spectrum was obtained (Figure 5).

Design, synthesis and characterization of DUPA-targeted and non-targeted HPMA copolymer-DTX conjugates

RAFT polymerization has been widely applied for the preparation of drug delivery systems due to its unique advantages: precise control of the molecular weight of the product, less by-products, opportunity to synthesize telechelic polymers and possibility to polymerize in aqueous environment [42]. The DUPA-targeted and non-targeted HPMA copolymer-DTX conjugates were prepared by RAFT polymerization of comonomers: MA-GFLG-DTX, MA-EG_{12}-DUPA and HPMA for P-DTX-EG_{12}-DUPA; MA-GFLG-DTX, MA-DUPA and HPMA for P-DTX-DUPA and P-DTX-mDUPA; MA-GFLG-DTX and HPMA for P-DTX. The schematic structure of all HPMA copolymer-DTX conjugates is shown in Figure 6. Figure 7 shows the structure and synthetic scheme of P-DTX-EG_{12}-DUPA. CPAD and V-65 were used as the chain transfer agent and initiator, respectively. The structure, synthetic scheme and SEC profile of P-DTX, P-DTX-DUPA and P-DTX-mDUPA are shown in Figures 5S, 6S and 7S, respectively. Table 1 summarizes the molecular weights, polydispersities, DTX and DUPA content in DUPA-targeted and non-targeted HPMA copolymer-DTX conjugates. The molecular weights of all polymer conjugates are well controlled with low polydispersities.

In vitro cytotoxicity

To check whether the C4-2 cell lines are PSMA positive, C4-2 prostate cancer cells and the negative control PC-3 prostate cancer cells were successively incubated with primary

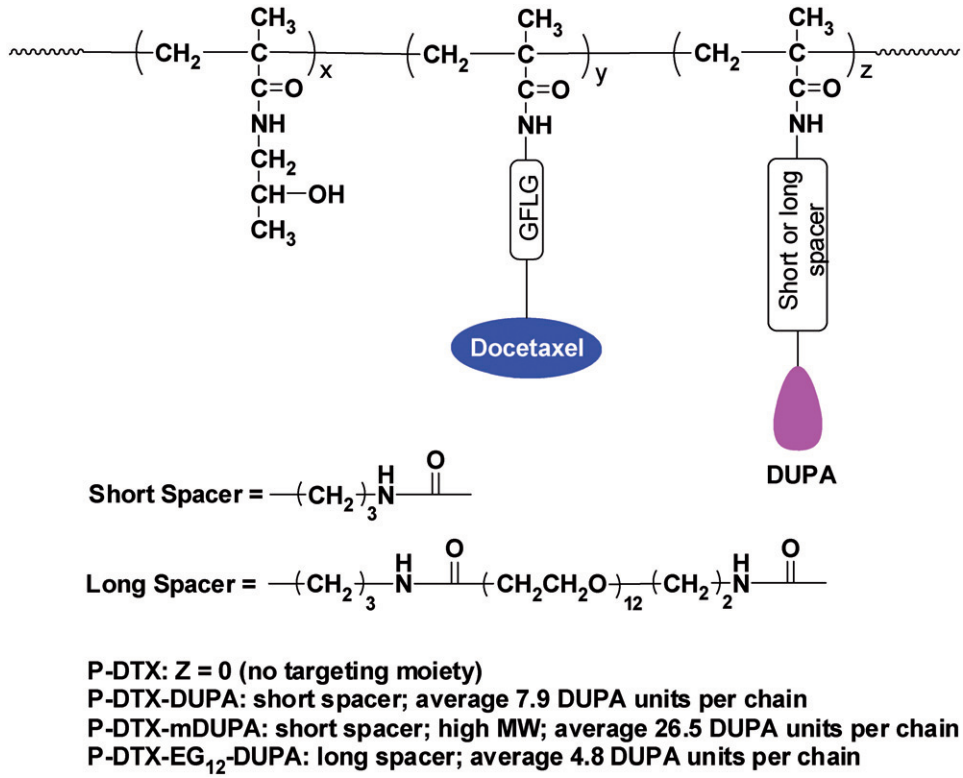

Figure 6. Schematic representation of the structure of DUPA-targeted DTX drug conjugates. See Table 1 for detailed characteristics of the conjugates.

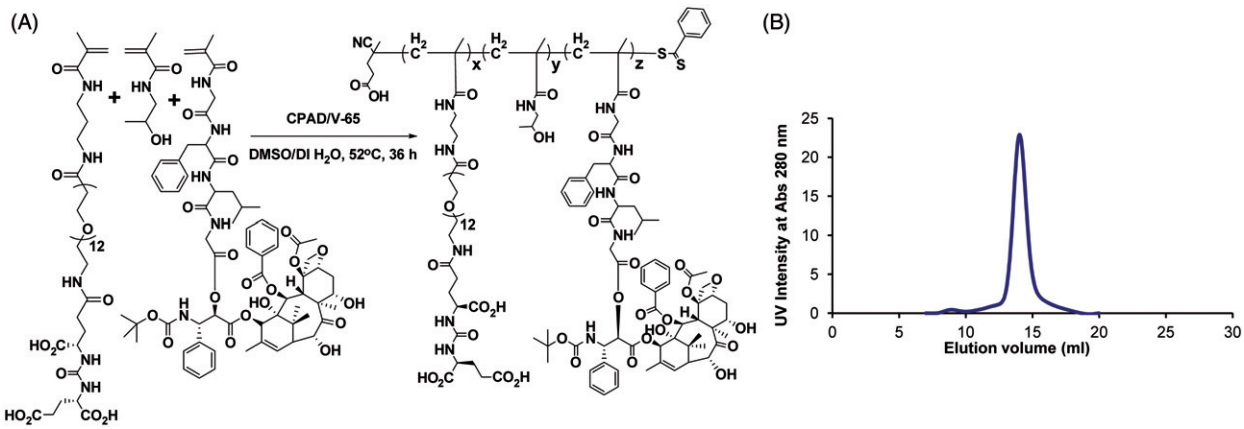

Figure 7. (A) Structure and synthetic scheme of P-DTX-EG_{12}-DUPA. (B) SEC profile of P-DTX-EG_{12}-DUPA (Mw 81 kDa).

mouse anti-PSMA human antibody and secondary goat anti-mouse IgG (H + L) antibody with Alexa Fluor 488. Then those cells were analyzed by flow cytometry. Unstained cells were used as the control. In Figure 8S, the red line indicates the unstained cells and the blue line indicates the stained cells. The flow cytometry results show that PSMA are expressed on C4-2 cells but not on PC-3. After confirmation of the PSMA cell surface expression on C4-2 cells, we evaluated the in vitro cytotoxicity of DUPA-targeted and non-targeted HPMA copolymer-DTX conjugates toward C4-2 human prostate cancer cells. As shown in Table 2, P-DTX, P-DTX-DUPA, P-DTX-mDUPA and P-DTX-EG_{12}-DUPA all possess strong cytotoxicity toward C4-2 cells ($IC_{50} = 4.14 \pm 1.03$ nM, 2.99 ± 1.09 nM, 3.32 ± 1.00 nM, 3.18 ± 0.42 nM, respectively. The data are presented as mean ± SEM. $n = 3$). The similar IC_{50} doses can be explained by the presence of ester bond between DTX and HPMA copolymer backbone; part of the DTX was released from the conjugates during 72 h incubation in cell culture media. Consequently, C4-2 cells were exposed to a mixture of free and polymer-bound DTX. This is consistent with other research group's results [43].

Table 2. IC_{50} of DUPA-targeted or non-targeted DTX conjugates against C4-2 prostate cancer cells.

	P-DTX	P-DTX-DUPA	P-DTX-mDUPA	P-DTX-EG_{12}-DUPA
IC_{50} (nM)	4.14 ± 1.03	2.99 ± 1.09	3.32 ± 1.00	3.18 ± 0.42

In vivo efficacy

Among prostate cancer tumor models, the C4-2 tumor model mimics closely human prostate cancer growth [44]. Therefore the antitumor activities of DUPA-targeted and non-targeted

HPMA copolymer-DTX conjugates were tested in six groups nu/nu mice bearing C4-2 prostate cancer xenografts ($n = 4$–6): untreated control (saline), free DTX, non-targeted conjugate (P-DTX) and DUPA-targeted conjugates (P-DTX-DUPA, P-DTX-mDUPA and P-DTX-EG_{12}-DUPA). Based on preliminary experiments, dosage (3 mg/kg) was enough to control C4-2 tumor growth (unpublished data). Three doses of 3 mg/kg DTX equivalent were administered *via* tail vein once per week (days 0, 7 and 14). At study end points, mice were euthanized and their tumors as well as organs were excised. As shown in Figure 8(A), the targeted DTX conjugate with longer spacer (P-DTX-EG_{12}-DUPA) was significantly more efficacious in tumor size reduction than P-DTX-DUPA, P-DTX-mDUPA, P-DTX, free DTX and saline. Typical images of excited tumors at the end points for DTX conjugate-treated groups are shown in Figure 8(B). For the treated group of P-DTX, P-DTX-mDUPA and P-DTX-EG_{12}-DUPA at day 42 after the first treatment, the mean relative tumor percent ((final tumor size/initial size)*100) were $(1590 \pm 208)\%$, $(1193 \pm 285)\%$ and $(810 \pm 160)\%$, respectively (mean ± SEM). Consistent with our hypothesis that the spacer length is important for DUPA attachment to the PSMA binding site, the efficacy of P-DTX-EG_{12}-DUPA was the highest of all conjugates studied. The length of the spacer in the latter is ~46 Å, thus DUPA may reach the binding site via a ~20 Å funnel-shaped tunnel [35] easier than conjugates with a short spacer. There was no significant difference in the efficacy of P-DTX, P-DTX-DUPA and P-DTX-mDUPA. Interestingly, the P-DTX-mDUPA possessed lesser efficacy than that P-DTX at early stages, but more efficacy in later stages of the experiment although the difference is not statistically significant.

Adverse effects

To evaluate whether the DUPA-targeted or non-targeted DTX conjugates have non-specific toxicities, the weight of treated and non-treated mice was monitored everyday. As shown in Figure 9, both treated and non-treated mice exhibited a slight weight loss maybe due to the bearing of tumor. However, there was no significant difference between treated and non-treated mice groups.

To further test whether the DTX conjugates have toxicity or not, we analyzed the histology of major organs (heart, liver, spleen, kidney, lung) after the mice were sacrificed. As shown in Figure 10, histologic examination of H&E stained sections from paraffin-embedded tissue of organs in treated and non-treated groups indicated no pathologic changes or end organ damage. Histologic sections from the heart and liver showed cadiomyocytes and hepatocytes within normal limits compared to saline-treated control samples. White and red bulb of the spleen also did not show histopathologic differences. Similarly, section of the kidney showed normal glomeruli without evidence of tubular necrosis in any of the groups. Compare to control group, there was no significant histologic difference in the lung tissue from the treated group.

Conclusions

In summary, we examined the targeting effect of DUPA and the spacer length effect in the treatment of PSMA expressing prostate cancer. Two polymerizable forms of DUPA with different spacer length have been prepared and characterized. DUPA-targeted and non-targeted HPMA copolymer – DTX conjugates with well-controlled molecular weight and molecular weight distribution were efficiently prepared by

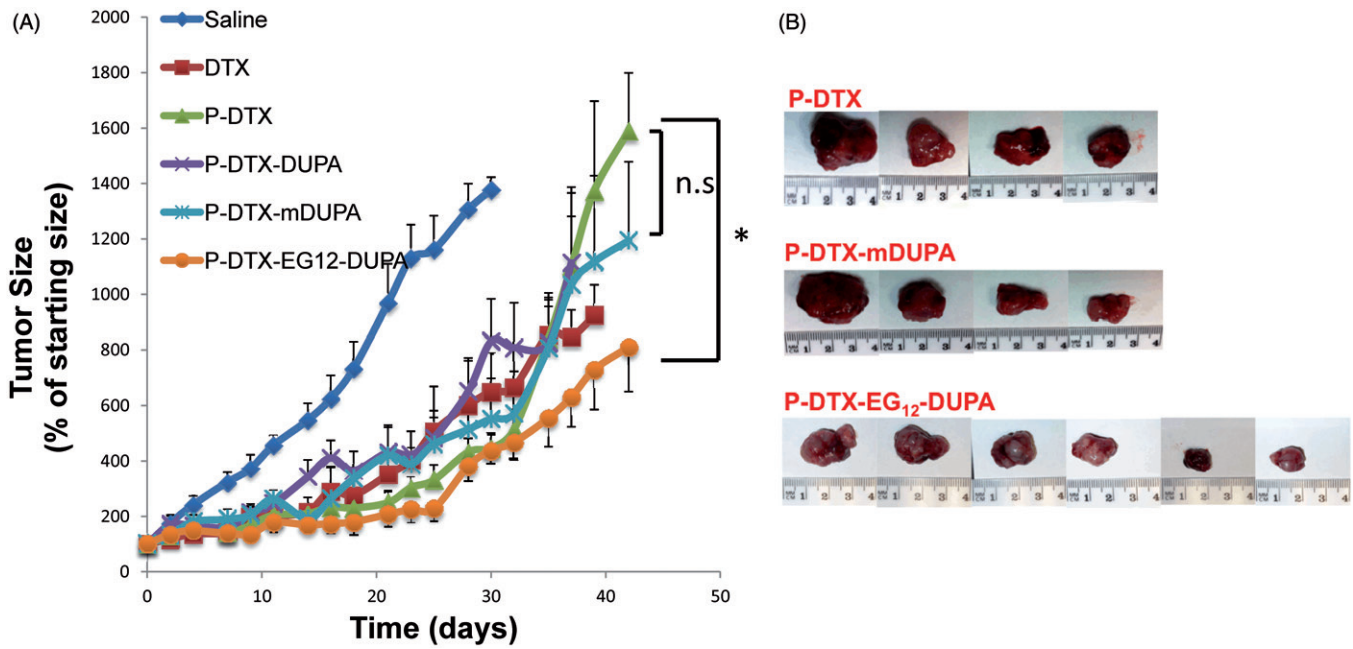

Figure 8. *In vivo* antitumor activity of DUPA-targeted or non-targeted HPMA copolymer-DTX conjugates in nude mice bearing s.c. C4-2 prostate cancer xenografts. (A) C4-2 tumor growth curve after treatment with three doses of DTX, P-DTX, P-DTX-DUPA, P-DTX-mDUPA and P-DTX-EG_{12}-DUPA (3 mg equivalent DTX/kg at days 0, 7 and 14). Control mice were administered saline. The data are presented as mean ± SEM ($n = 4$–6; $^*p < 0.05$; ns, not significant). (B) Images of excised tumors from mice, which were treated by P-DTX, P-DTX-mDUPA and P-DTX-EG_{12}-DUPA, respectively. Those mice were sacrificed at day 42 after the first injection.

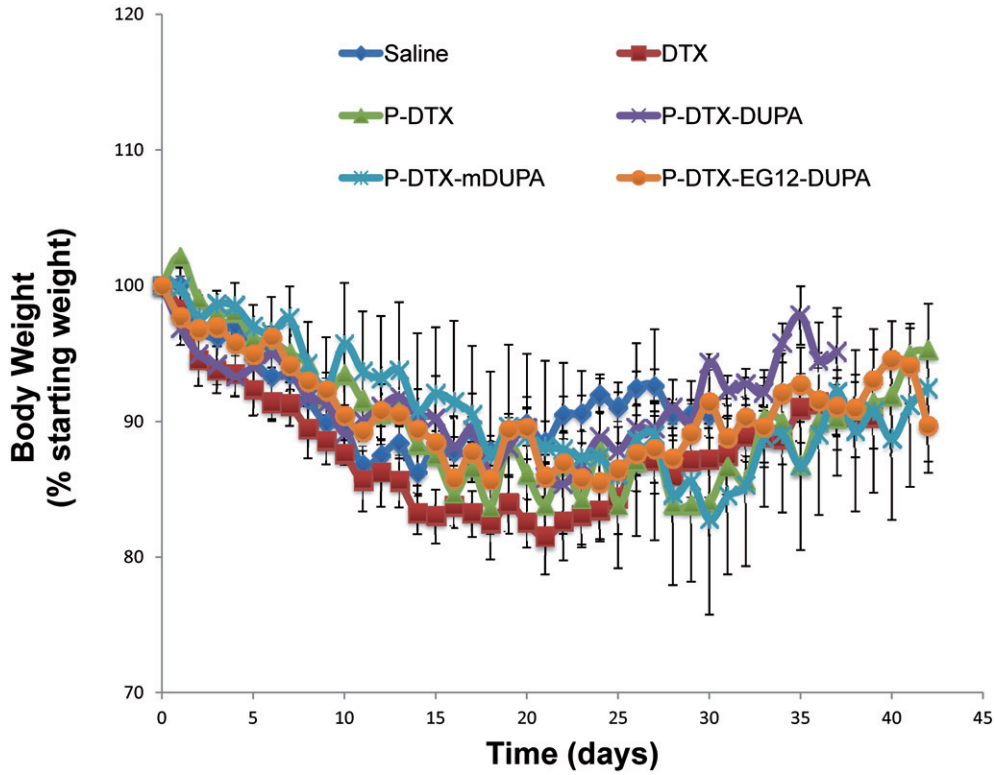

Figure 9. Percentage of mean body weight change of nu/nu mice bearing s.c. C4-2 prostate cancer xenografts following administration of saline, DTX, P-DTX, P-DTX-DUPA, P-DTX-mDUPA and P-DTX-EG_{12}-DUPA (3 mg equivalent DTX/kg at days 0, 7 and 14). The data are presented as mean ± SEM ($n = 4$–6).

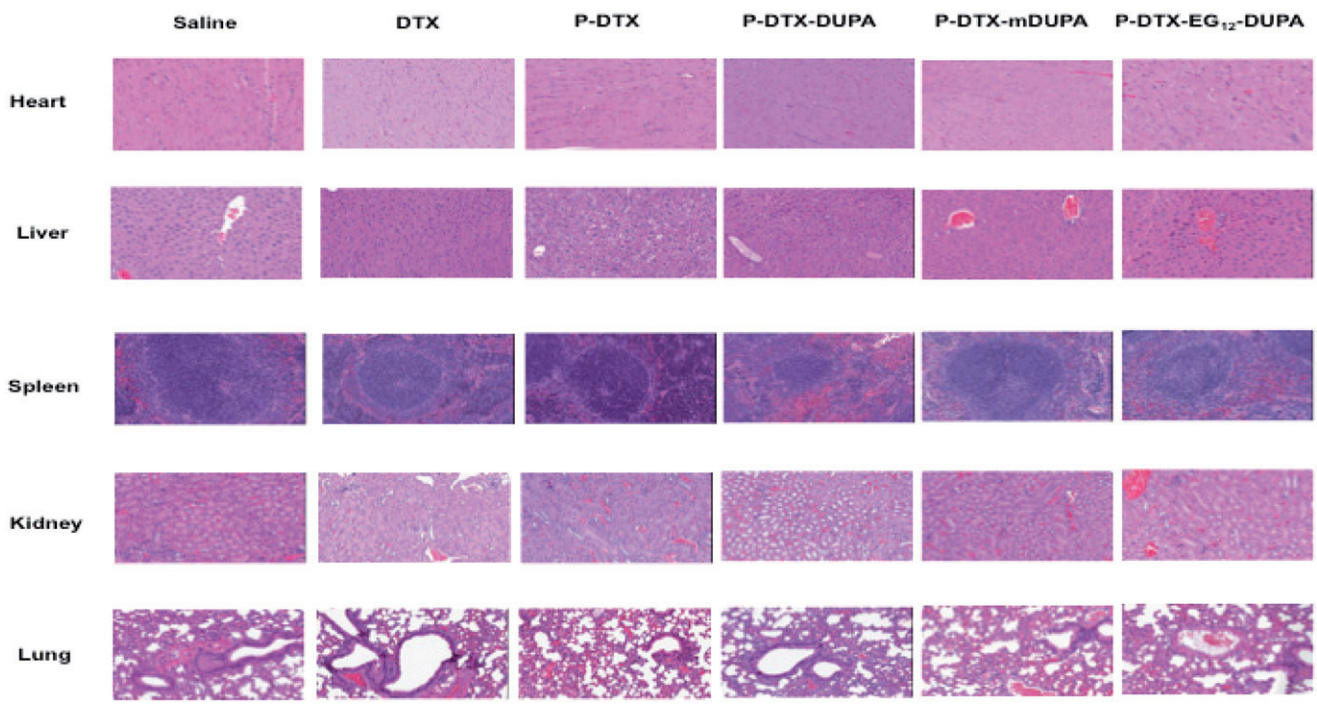

Figure 10. Histology images of major organs (heart, liver, spleen, kidney, lung) from control and treated mice.

RAFT polymerization. To our knowledge, this is the first time where the targeting moiety DUPA was directly incorporated into drug delivery system by polymerization. Importantly, the general approach to prepare monomer form of DUPA can be extended to a wide variety of other PSMA-targeting moieties such as phosphoramidates and peptides. Importantly, the P-DTX-mDUPA and P-DTX-EG_{12}-DUPA-treated groups exhibited better tumor regression than that of the P-DTX-treated group at the study end point. This might be attributed to the targeting effect of DUPA toward PSMA on tumor cells. Furthermore, P-DTX-EG_{12}-DUPA exhibited better C4-2 tumor regression than that of P-DTX-mDUPA

even though the P-DTX-mDUPA contains more targeting moieties than P-DTX-EG_{12}-DUPA. These *in vivo* results show that the spacer length between targeting moieties and HPMA copolymer backbone affects the DUPA's targeting effect, and concomitantly the treatment efficacy of DTX conjugates against C4-2 tumor-bearing nu/nu mice. However, it is also possible that the enhanced treatment effect of P-DTX-EG_{12}-DUPA result from other factors such as the change of morphology and enhanced water solubility of conjugates. Moreover, histology study showed that the DUPA-targeted DTX conjugate exhibited no non-specific toxicity to the treated mice. This formulation design provides a promising targeted therapeutics for PSMA expressing prostate cancer treatment. The DUPA-targeted DTX conjugates in this study may prove the importance of spacer length in targeted drug delivery, especially when the size of targeting moiety is small. Further modifications, such as optimizing the targeting moieties distribution and increasing the number of targeting moieties per polymer chain, should further enhance the DUPA targeting effect.

Acknowledgements

We thank members of Dr Kopeček's laboratory for helpful discussions and technical support and Dr Elsässer-Beile for providing the C4-2 tumor cell line and the 3 F/11 antibody. We acknowledge Karthik Raman in Dr Balagurunathan's group and Vasudev Bhonde in Dr Looper's group for help with using the microwave instruments.

Declaration of interest

This work is a part of PhD thesis of Zheng-hong Peng at University of Utah. This work was supported in part by NIH through grant RO1 CA132831.

References

1. Siegel R, Naishadham D, Jemal A. Cancer statistics. CA Cancer J Clin 2013;63:11–30.
2. Olson WC, Heston WDW, Rajasekaran AK. Clinical trials of cancer therapies targeting prostate-specific membrane antigen. Rev Recent Clin Trials 2007;2:182–90.
3. Siegel R, Desantis C, Virgo K, et al. Cancer treatment and survivorship statistics. CA Cancer J Clin 2012;62:220–41.
4. Tannock IF, Wit R, Berry WR, et al. Docetaxel plus prednisone or mitoxantrone plus prednisone for advanced prostate cancer. N Engl J Med 2004;351:1502–12.
5. Davis ME, Chen Z, Shin DM. Nanoparticle therapeutics: an emerging treatment modality for cancer. Nat Rev Drug Disc 2008;7:771–82.
6. Duncan R. Polymer conjugates as anticancer nanomedicines. Nat Rev Cancer 2006;6:688–701.
7. Kopeček J. Polymer–drug conjugates: origins, progress to date and future directions. Adv Drug Delivery Rev 2013;65:49–59.
8. Kopeček J, Kopečková P. Design of polymer-drug conjugates. In: Kratz F, Senter P, Steinhagen H, eds. Drug delivery in oncology, Vol. 2, Chapter 17. Weinheim, Germany: Wiley-VCH; 2012:485–512.
9. Yu MK, Park J, Jon S. Targeting strategies for multifunctional nanoparticles in cancer imaging and therapy. Theranostics 2012;2:3–44.
10. Zhou Y, Kopeček J. Biological rationale for the design of polymeric anticancer nanomedicines. J Drug Target 2013;21:1–26.
11. Schulke N, Varlamova OA, Donovan GP, et al. The homodimer of prostate-specific membrane antigen is a functional target for cancer therapy. Proc Natl Acad Sci USA 2003;100:12590–5.
12. Israeli, RS, Powell CT, Corr JG, et al. Expression of the prostate-specific membrane antigen. Cancer Res 1994;54:1807–11.
13. Ghosh A, Heston WDW. Tumor target prostate specific membrane antigen (PSMA) and its regulation in prostate cancer. J Cell Biochem 2004;91:528–39.
14. Ross JS, Sheehan CE, Fisher HA, et al. Correlation of primary tumor prostate-specific membrane antigen expression with disease recurrence in prostate cancer. Clin Cancer Res 2003;9:6357–62.
15. Ni X, Zhang Y, Ribas J, et al. Prostate-targeted radiosensitization via aptamer-shRNA chimeras in human tumor xenografts. J Clin Invest 2011;121:2383–90.
16. Dassie JP, Liu XY, Thomas GS, et al. Systemic administration of optimized aptamer-siRNA chimeras promotes regression of PSMA-expressing tumors. Nat Biotechnol 2009;27:839–46.
17. Bagalkot V, Farokhzad OC, Langer R, Jon S. An aptamer-doxorubicin physical conjugate as a novel targeted drug-delivery platform. Angew Chem Int Ed 2006;45:8149–52.
18. Elsässer-Beile U, Reischl G, Wiehr S, et al. PET imaging of prostate cancer xenografts with a highly specific antibody against the prostate-specific membrane antigen. J Nucl Med 2009;50:606–11.
19. Evans MJ, Smith-Jones PM, Wongvipat J, et al. Noninvasive measurement of androgen receptor signaling with a positron-emitting radiopharmaceutical that targets prostate-specific membrane antigen. Proc Natl Acad Sci USA 2011;108:9578–82.
20. Henry MD, Wen S, Silva MD, et al. A prostate-specific membrane antigen targeted monoclonal antibody chemotherapeutic conjugates designed for the treatment of prostate cancer. Cancer Res 2004;64:7995–8001.
21. Moffatt S, Papasakelariou C, Wiehle S, Cristiano R. Successful in vivo tumor targeting of prostate-specific membrane antigen with a highly efficient J591/PEI/DNA molecular conjugate. Gene Therapy 2006;13:761–72.
22. Aggarwal S, Singh P, Topaloglu O, et al. A dimeric peptide that binds selectively to prostate-specific membrane antigen and inhibits its enzymatic activity. Cancer Res 2006;66:9171–7.
23. Rege K, Patel SJ, Megeed Z, Yarmush ML. Amphipathic peptide-based fusion peptides and immunoconjugates for the targeted ablation of prostate cancer cells. Cancer Res 2007;67:6368–75.
24. Kularatne SA, Wang K, Santhapuram HKR, Low PS. Prostate-specific membrane antigen targeted imaging and therapy of prostate cancer using a PSMA inhibitor as a homing ligand. Mol Pharmaceutics 2009;6:780–9.
25. Kularatne SA, Venkatesh C, Santhapuram HKR, et al. Synthesis and biological analysis of prostate-specific membrane antigen-targeted anticancer prodrugs. J Med Chem 2010;53:7767–77.
26. Sanna V, Pintus G, Bandiera P, et al. Development of polymeric microbubbles targeted to prostate-specific membrane antigen as prototype of novel untrasound contrast agents. Mol Pharmaceutics 2011;8:748–57.
27. Banerjee SR, Pullambhatla M, Byun Y, et al. Sequential SPECT and optical imaging of experimental models of prostate cancer with a dual modality inhibitor of the prostate-specific membrane antigen. Angew Chem Int Ed 2011;50:9167–70.
28. Humblet V, Misra P, Bhushan KR, et al. Multivalent scaffolds for affinity maturation of small molecule cell surface binders and their application to prostate tumor targeting. J Med Chem 2009;52:544–50.
29. Maresca KP, Hillier SM, Femia FJ, et al. A series of halogenated heterodimeric inhibitors of prostate specific membrane antigen (PSMA) as radiolabeled probes for targeting prostate cancer. J Med Chem 2009;52:347–57.
30. Liu T, Nedrow-Byers JR, Hopkins MR, Berkman CE. Spacer length effects on in vitro imaging and surface accessibility of fluorescent inhibitor of prostate specific membrane antigen. Bioorg Med Chem 2011;21:7013–16.
31. Zhou J, Neale JH, Pomper MG, Kozikowski AP. NAAG peptidase inhibitors and their potential for diagnosis and therapy. Nat Rev Drug Disc 2005;4:1015–25.
32. Jayaprakash S, Wang X, Heston WD, Kozikowski AP. Design and synthesis of a PSMA inhibitor-doxorubicin conjugate for targeted prostate cancer therapy. ChemMedChem 2006;1:299–302.
33. Zhang AX, Murelli RP, Barinka C, et al. A remote arene-binding site on prostate specific membrane antigen revealed by antibody-recruiting small molecules. J Am Chem Soc 2010;132:12711–16.

34. Davis MI, Bennett MJ, Thomas LM, Bjorkman PJ. Crystal structure of prostate-specific membrane antigen, a tumor marker and peptidase. Proc Natl Acad Sci USA 2005;102:5981–6.
35. Mesters JR, Barinka C, Li W, et al. Structure of glutamate carboxypeptidase II, a drug target in neuronal damage and prostate cancer. EMBO J 2006;25:1375–84.
36. Kopeček J, Kopečková, P. HPMA copolymers: origins, early developments, present, and future. Adv Drug Delivery Rev 2010; 62:122–49.
37. Kopeček J, Bažilová H. Poly[*N*-(2-hydroxypropyl)methacrylamide]. 1. Radical polymerization and copolymerization. Eur Polym J 1973;9:7–14.
38. Rejmanová P, Pohl J, Baudyš M, et al. Polymers containing enzymatically degradable bonds. 8. Degradation of oligopeptide sequences in *N*-(2-hydroxypropyl)methacrylamide copolymers by bovine spleen cathepsin B. Makromol Chem 1983;184:2009–20.
39. Mitsukami Y, Donovan MS, Lowe AB, McCormick CL. Water-soluble polymers. 81. Direct synthesis of hydrophilic styrenic-based homopolymers and block copolymers in aqueous solution via RAFT. Macromolecules 2001;34:2248–56.
40. Satchi-Fainaro R, Puder M, Davies JW, et al. Targeting angiogenesis with a conjugate of HPMA copolymer and TNP-470. Nat Med 2004;10:255–61.
41. Liu J, Kopečková, P, Pan H, et al. Prostate cancer targeted N-(2-hydroxypropyl)methacrylamide copolymer/docetaxel conjugates. Macromol Biosci 2012;12:412–22.
42. York AW, Kirkland SE, McCormick CL. Advances in the synthesis of amphiphilic block copolymers via RAFT polymerization: stimuli-responsive drug and gene delivery. Adv Drug Delivery Rev 2008;60:1018–36.
43. Etrych T, Šírová M, Starovoytova L, et al. HPMA copolymer conjugates of paclitaxel and docetaxel with pH-controlled drug release. Mol Pharmaceutics 2010;7:1015–26.
44. Thaimann GN, Anezinis PE, Chang SM, et al. Androgen-independent cancer progression and bone metastasis in the LNCaP model of human prostate cancer. Cancer Res 1994;54: 2577–81.

Supplementary material available online

Supplementary Figures 1–8